nature communications

Article

https://doi.org/10.1038/s41467-025-67153-1

Sequestration of the phagocyte metabolite itaconate by *Pseudomonas aeruginosa* RpoN promotes successful pulmonary infection

Received: 31 July 2025

Accepted: 20 November 2025

Published online: 13 December 2025

Check for updates

Ayesha Z. Beg[1], Zihua Liu[2,3], Ying-Tsun Chen[1], Absar Talat[4], Griffin Gowdy[1], Jake Miller[1], Lindsey Florek[5], Lars Dietrich[6], Chu Wang[1,2], Ian Lewis[6], Tania Wong Fok Lung[7], Sebastian Riquelme[1] & Alice Prince[1]

Inhaled opportunistic pathogens such as *Pseudomonas aeruginosa* actively modify gene expression to meet the challenges of a new environment. In the infected airway the bacteria must respond to the immunometabolite itaconate, which is abundantly produced by macrophages and has anti-inflammatory and anti-oxidant functions that protect the host from airway damage and causes toxicity to bacteria. As a dicarboxylate that targets cysteine residues, itaconate can modify both bacterial and host proteins often altering metabolic activity. We demonstrate that itaconate promotes a global metabolic response in *P. aeruginosa* by enhancing the activity of the major alternative transcription factor RpoN. Itaconate is actively transported into the bacteria, induces σ^{54} rpoN expression and covalently binds cysteine residues 218 and 275 on RpoN helping to neutralize its toxicity. The S-itaconated RpoN exhibits a gain of function driving increased glucose catabolism and enhanced utilization of the bioenergetically efficient Entner–Doudoroff pathway. Thus, the accumulation of itaconate in the infected airway promotes the adaptation of *P. aeruginosa* to the lung by optimizing its metabolic activity and ability to cause pneumonia.

E*SKAP*E (*Enterococcus faecium*, *Staphylococcus aureus*, *Klebsiella pneumoniae*, *Acinetobacter baumannii*, *Pseudomonas aeruginosa*, and *Enterobacter* spp.) pathogens, such as *P. aeruginosa*, whether antibiotic resistant or not, are a major cause of health care associated pneumonia world wide[1]. They are typically aspirated into the lung from abiotic sites such as puddles, showers, or sinks and must rapidly adapt or risk immune clearance. To establish a nidus of infection, successful opportunists evade a variety of host antibacterial effectors. They must optimize metabolic activity, selecting from the abundant carbon sources available, but without fueling excessive growth that would elicit an immune response toxic to both host and pathogen[2]. We wanted to understand how these bacteria sense they are in a human airway and coordinate gene expression to enable proliferation in response to this specific environmental challenge.

Both classical and alternative sigma factors coordinate bacterial sensing and adaptation to diverse environments. The alternative σ^{54} factor RpoN is among the over 400 *P. aeruginosa* transcriptional regulators that control bacterial gene expression in response to local cues.

[1]Department of Pediatrics, Columbia University, New York, NY, USA. [2]Synthetic and Functional Biomolecules Center, College of Chemistry and Molecular Engineering, Peking University, Beijing, China. [3]Peking-Tsinghua Center for Life Sciences, Academy for Advanced Interdisciplinary Studies, Peking University, Beijing, China. [4]Antimicrobial Resistance Lab, Interdisciplinary Biotechnology Unit, AM University, Aligarh, India. [5]Dept. of Biological Sciences, Columbia University, New York, NY, USA. [6]Department of Biological Sciences, University of Calgary, Calgary, AB, Canada. [7]Department of Microbiology, Biochemistry & Molecular Genetic, Center for Immunity and Inflammation, Rutgers NJ Medical School, Newark, NJ, USA. e-mail: asp7@columbia.edu

https://doi.org/10.1038/s41467-025-67153-1

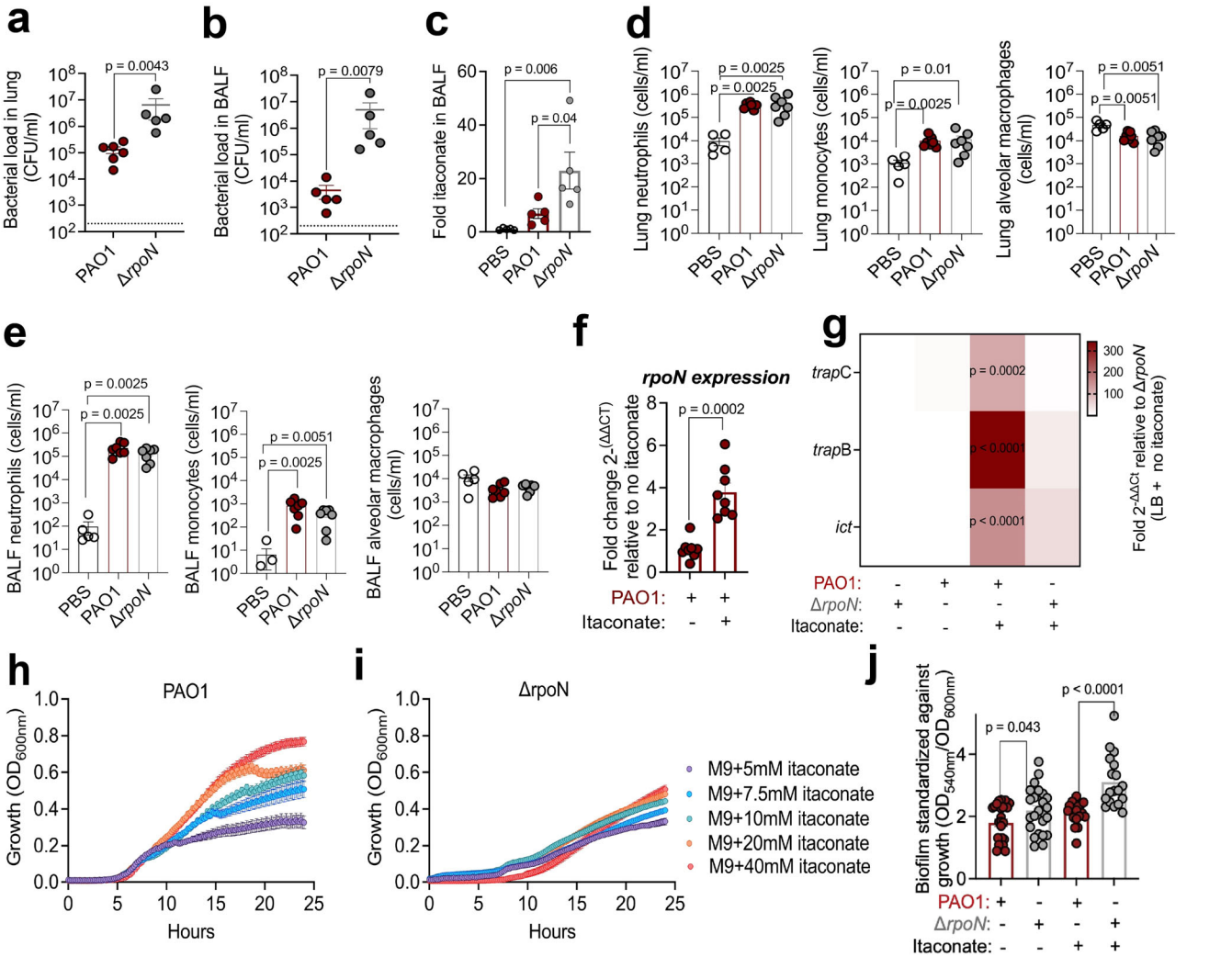

Fig. 1 | Expression of *rpoN* regulates bacterial pathogenesis and response to itaconate. a–e Characteristics of acute pulmonary infection in C57 BL/6NJ mice following intranasal inoculation of WT or Δ*rpoN* PAO1 strains at 16 h post-infection. Bacterial burden from **a** lung and **b** Broncheoalveaolar lavage fluid (BALF) ($n = 3$, with total 5 mice per group). **c** Relative abundance of itaconate in the BALF normalized to the PBS group ($n = 3$, with total 5 mice per group). Immune cells in **d** BALF **e** lung ($n = 3$, with total 5–6 mice per group). **f–j** In vitro *rpoN*-mediated response to itaconate. RT-qPCR based quantification of **f** *rpoN* mRNA in PAO1 WT relative to itaconate ($n = 8$) and **g** itaconate metabolizing (*ict*) and transporter (*trap*B, *trap*C) genes in PAO1 WT relative to Δ*rpoN* +/− itaconate ($n = 6$) (*trap*B: $p < 0.0001 = 1E\text{-}07$; *ict*: $p < 0.0001 = 1.5E\text{-}07$). Growth curves of **h** PAO1 and **i** Δ*rpoN* PAO1 strains in M9 minimal media supplemented with increasing concentrations of itaconate (5–40 mM) as a sole carbon source ($n = 3$). **j** Biofilm production (normalized to growth) by WT and Δ*rpoN* PAO1 strains in LB media +/− itaconate at 24 h ($n = 12$–18) (LB+ itaconate-PAO1 WT or Δ*rpoN*, $p < 0.0001 = 5.4E\text{-}05$). Data are presented as mean ± s.e.m. Statistical significance was assessed unpaired Mann–Whitney *U t*-test (**a**, **b**, **d**–**f**), and One way ANOVA using Tukey's multiple comparison test with specific two-tailed unpaired *t*-test (**c**, **g**, **j**). ns non-significant. All statistical tests are two-sided. Source data are provided as a Source Data file 1.

RpoN is involved in both the positive and negative regulation of genes that influence bacterial persistence in the respiratory tract, including multiple quorum sensing systems, biofilm formation, motility, and especially metabolism[3–6]. As RpoN directs pathways involved in the uptake and assimilation of desirable carbon sources to generate energy, it seemed likely that this transcription factor plays a major role in bacterial adaptation to the environment imposed by the infected airway.

Itaconate, synthesized by immunoresponsive gene 1 (*Irg1*), is a major airway metabolite released by phagocytes in response to infection[7]. It modifies both host and bacterial proteins through covalent interactions with specific cysteine residues, often altering metabolic activities[8–10]. In the host, Itaconate shapes immunoregulatory processes via *S*-itaconation of proteins involved in pro-inflammatory signaling, such as the NLRP3 inflammasome, the Nrf2-sequestrator Keap1, and succinate dehydrogenase. In bacteria Itaconate is toxic[11,12] and acts as an electrophile, inducing substantial membrane stress as well as blocking TCA cycle function and inhibiting carbohydrate catabolism, particularly glycolysis[13,14]. As one of the most abundant metabolites in the infected airway, we postulated that itaconate serves as a host-specific signal that stimulates *P. aeruginosa* to adapt to the lung environment. In the experiments detailed in this report, we demonstrate how the binding of itaconate at two highly conserved cysteine residues in RpoN sequesters this electrophile and modifies RpoN function to promote *P. aeruginosa* carbohydrate catabolism, fueling bacterial adaptation to the lung.

Results

RpoN directs *P. aeruginosa* responses to itaconate in the lung

P. aeruginosa pulmonary infection elicits a brisk phagocytic response, dominated by their abundant release of itaconate[14]. To directly test the impact of RpoN-dependent transcription on *P. aeruginosa* in vivo, we compared the outcomes of pulmonary infection in mice exposed to the WT PAO1 strain or a Δ*rpoN* mutant, appreciating that over 400

genes are under either positive or negative RpoN regulation[15]. The Δ*rpoN* strains achieved a higher bacterial load than the WT PAO1 (Fig. 1a, b) and stimulated slightly greater levels of IL-1a, IL-1b, MIG, and MCP-1, but not IL-6 or TNFa (Supplementary Fig. 1a), consistent with the increased bacterial load. Mice infected with WT PAO1 exhibited decreased amounts of itaconate in the airway (Fig. 1c) yet had similar numbers of phagocytes, the cells that produce itaconate (Fig. 1d, e). The apparent ability of WT bacteria to limit the accumulation of itaconate in the airways could be either a bacterial or host effect. Taken together, these results suggested to us that RpoN may interact with itaconate specifically in its response to the airway metabolome.

We observed that the organisms respond to itaconate by increasing *rpoN* mRNA expression, as well as expression of the itaconate transporters *trap*B, *trap*C, and *ict* involved in itaconate assimilation[16] (Fig. 1f, g); suggesting that the pathogen employs *rpoN* as both sensor and defense mechanism in response to the immunometabolite. In vitro in the presence of itaconate *rpoN* expression protects *P. aeruginosa* proliferation (Fig. 1h). Whereas, the Δ*rpoN* mutant exhibits decreased growth rate (Fig. 1i) but increased production of biofilm in response to itaconate stress (Fig. 1j). Transcriptional studies confirmed that the Δ*rpoN* mutant responded to itaconate with increased expression of the families of genes involved in quorum sensing (*las*, *rhl)* and biofilm formation (*psl*, *pel*, alginate), mechanisms to protect against oxidant stress (Supplementary Fig. 1b). These studies indicate the physiological relevance of RpoN for *P. aeruginosa* adaptation to an itaconate-rich environment like the lung. We next addressed how RpoN and itaconate might interact to regulate *P. aeruginos*a adaptation to the lung.

RpoN S-itaconation sequesters itaconate and enhances *P. aeruginosa* persistence-

As an electrophile, itaconate can function as a non-specific oxidant, but it also has a major role in post-translational modification of specific targets by covalently binding available cysteine residues—i.e., S-itaconation; modifications that can result in either loss or gain of function[17]. The conserved cysteine residues in *P. aeruginosa* PAO1 RpoN at 218 and 275 are sites of *S*-itaconation identified using a biorthogonal probe (C3A) validated for itaconate (Fig. 2a and Supplementary Fig. 2a)[10]. We postulated that *S*-itaconation of RpoN at these two cysteine residues is a key factor responsible for *P. aeruginosa* to thrive in the host lung.

We compared the outcomes of infection using *P. aeruginosa* strains with mutated *rpo*N lacking expression of the key cysteine residues that are itaconated versus the native *rpo*N. We complemented the PAO1 Δ*rpoN* mutant strain with a plasmid expressing either WT*rpoN* or an *rpoN* gene in which the cysteine residues at 218 and 275 were replaced with alanines and thus unable to be *S*-itaconated[18] (Fig. 2b). For simplicity of notation, PAO1 Δ*rpoN* complemented with plasmid encoding WT *rpoN* is referred to as "WT*rpoN*" in contrast to PAO1 Δ*rpo*N expressing plasmid encoding C218/275A mutant *rpoN*, referred to as "C218/275A". *P. aeruginosa* harboring RpoN available for *S*-itaconation, whether chromosomal or plasmid mediated, had equivalent ability to sense the immunometabolite pressure in vivo and in vitro, as shown by similar levels of murine infection (Supplementary Fig. 2b) and biofilm formation (Supplementary Fig. 2c). We predicted that C218/275A, lacking the cysteine residues essential for itaconate binding, would exhibit biologically relevant phenotypes specifically in the presence of itaconate, but appreciated that other RpoN functions that are itaconate independent might be affected by the cysteine to alanine mutations. Phenotypic comparison revealed a slight growth advantage of the C218/275 A mutant over WT*rpoN* when itaconate or succinate were used as sole carbon sources, whereas growth in glucose was inhibited by itaconate (Supplementary Fig. 2d–f). Aside from these differences, both WT*rpoN* and C218/275A had equivalent rates of oxygen consumption and swarming motility, which are under RpoN regulation (Supplementary Fig. 2g, h).

In vivo, RpoN *S*-itaconation supported *P. aeruginosa* survival in the respiratory tract. Compared with animals exposed to the C218/275A mutant, lungs of mice infected with the WT*rpoN* strain exhibited increased bacterial burden (Fig. 2c, d). This increased infection was dependent upon the presence of itaconate as both WT*rpoN* and the C218/275A mutant strains achieved similar levels of infection in *Irg1*$^{-/-}$ animals lacking itaconate (Fig. 2c, d). In vitro, the C218/275A mutant was significantly impaired in biofilm production in response to itaconate (Fig. 2e, f). Importantly, the bacteria expressing RpoN capable of sensing the itaconate via cysteine modification as well as those with an alanine substitution, did not have significant alterations in other host effector responses against *P. aeruginosa*, such as their induction of itaconate production (Fig. 2g), stimulation of infiltrating phagocytes(Fig. 2h–j), or release of inflammatory cytokines (Supplementary Fig. 2i). Together, these findings strongly suggest that itaconate sequestration by RpoN via *S*-itaconation confers *P. aeruginosa* with major survival advantages in a phagocyte-dominated setting.

RpoN *S*-itaconation promotes glucose catabolism via the ED pathway

We anticipated that the protection conferred to *P. aeruginosa* by RpoN *S*-itaconation would involve mechanisms that promote the establishment of the bacterial biomass in the lung. Transcriptomic profiles of the WT*rpoN* and C218/275A mutant (Supplementary data 1) indicated several changes attributable to the C-A mutations under control conditions (Supplementary Fig. 3a, c), as well as marked differences in key pathways in the presence of itaconate (Fig. 3a and Supplementary Fig. 3b). While itaconate itself can be assimilated by *P.aeruginosa*[14], its preferred mechanism to generate ATP and other precursor molecules under conditions of oxidant stress is via the energetically efficient Entner–Doudoroff (ED) pathway (Fig. 3a)[19–22]. This prioritizes the allocation of glucose to a range of metabolic networks involved in the synthesis of antioxidants, such as NADP+, as well as anthranilate metabolism, quorum sensing, iron scavenging, and nucleotide synthesis all important for biomass expansion. We observed that itaconated RpoN was associated with significantly increased expression of *gcd*, which converts glucose to gluconate, as compared with the C218/275A mutant. Additionally, RpoN S-itaconation favored gluconate oxidation to ketogluconates and its utilisation via the ED pathway, particularly by preventing mRNA repression of *kgu*DET, *zwf*, *pgl*, and *eda* (Fig. 3c–e). There was also increased expression of the antranilates, *ant*ABC, which participate in the degradation of tryptophan via the kyrenurine pathway, which generates NAD^+ and $NADP^+$[23,24], cofactors needed to accept electrons in the production of gluconate and glycerol-3 phosphate via DHAP (Fig. 3a, b).

Using carbon tracing assays, we corroborated how RpoN *S*-itaconation facilitated *P. aeruginosa* [^{13}C]-glucose catabolism comparing the effects of itaconate on WT*rpoN* and C218/275 A mutants (Supplementary data 2). In the presence of itaconate, more of the [^{13}C] signature was integrated into specific isotopologues of NADP+, NAD+ and glycerol −3- phosphate (Fig. 3f–h) core elements on the ED pathway. There was significant [^{13}C] enrichment in nucleic acid precursors; uridine monopohosphate (UMP), 5-thymidylic acid (dTMP), and cytidine monophosphate (CMP) in WT*rpoN* as compared to C218/C275A as well (Fig. 3i–k). WT*rpoN* incorporated significantly more [^{13}C] into lipid and rhamnolipid precursors derived from acetylCoA, such as 2-hydroxycaproic acid and D-2-hydroxyglutaric acid (Supplementary Fig. 3g) and into the glycerolipid precursors glycerol-3 phosphate and O-phosphoethanolamine (Fig. 3h and Supplementary Fig. 3g). WT*rpoN* also incorporated more [^{13}C]-glucose into *N*-acetyl-glucosamine-1-phosphate (GlcNAc-1-P) and UDP-glucose (UDP-Glc)(Fig. 3l, m), essential components of peptidoglycan and biofilm.

We also observed changes in ^{13}C glucose flux attributed solely to C-A mutations (Supplementary Fig. 3e, f); namely decreased ^{13}C enrichment into guanine diphosphate, ornithine, alanine, asparagine

https://doi.org/10.1038/s41467-025-67153-1

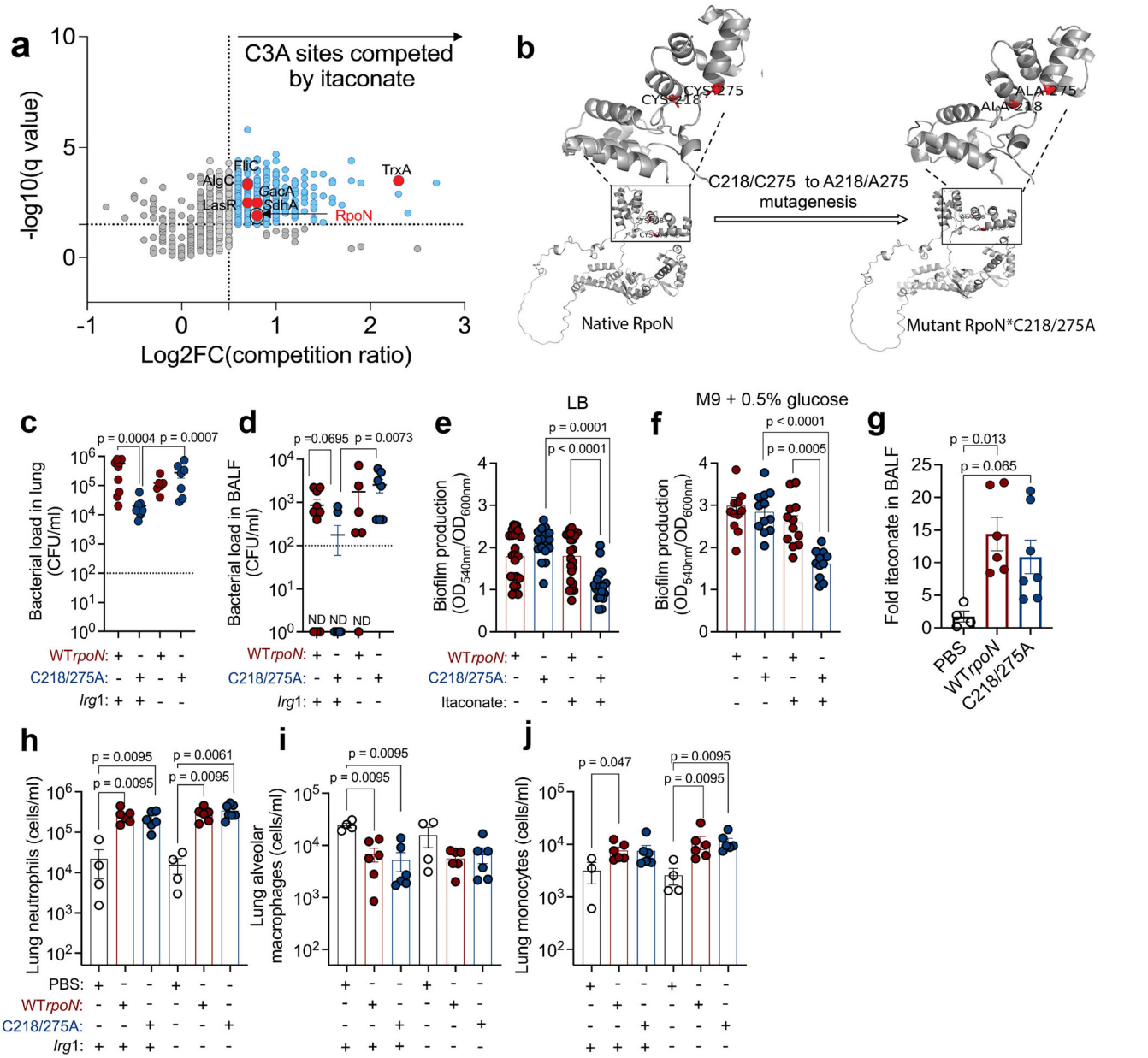

Fig. 2 | Impact of RpoN S-itaconation on *P. aeruginosa* pulmonary infection. **a** Identification of sites in live PAO1 WT that are labelled by C3A probe that are selectively competed by itaconate ($n = 3$). Thresholds for the itaconate log2FC competition ratio and $-\log_{10}$(*q*-value) are set at 0.5 and 1.5, respectively. Blue dots indicate sites increasingly competed by itaconate, while red dots highlight itaconated RpoN and common pathoadaptive proteins in *P. aeruginosa*. **b** Ribbon structure of RpoN highlighting substitution of C218 and C275 in native RpoN (red) to A218 and A275 in mutant RpoN (red). **c**, **d**, **g**–**j** Characteristics of acute pulmonary infection in C57 BL/NJ6 WT or Irg1 $^{-/-}$ mice following intranasal inoculation of WT*rpoN* or C218/275A PAO1 strains at 16 h post-infection. Bacterial burden from **c** lung, **d** BALF ($n = 3$, with total 7–9 mice per group). In vitro effects of itaconate on biofilm production (normalized to growth) by WT*rpoN* or C218/275A PAO1 in (**e**) LB media ($n = 18$) ($p < 0.0001 = 4.6E\text{-}07$) or **f** M9 media supplemented with 0.5% glucose at 24 h or 48 h ($n = 12$) ($p < 0.0001 = 2.6\ E\text{-}05$), respectively. **g** Relative abundance of itaconate in the BALF normalized to the PBS group ($n = 3$, with total 6 mice per group). **h** Neutrophils **i** alveolar macrophages **j** monocytes in lung ($n = 3$, with total 6–7 mice per group. Data are presented as mean ± s.e.m. Statistical significance was assessed using unpaired Mann–Whitney *U t*-test (**c**, **d**, **h**–**j**) and One way ANOVA using Tukey's multiple comparison test with specific two-tailed unpaired *t*-test (**e**–**g**). All statistical tests are two-sided. Source data are provided as a Source Data file 2.

and allantoin (Supplementary Fig. 3h), but increased ^{13}C incorporation into L-cystathione and niacinamide (Supplementary Fig. 3i). The ^{13}C incorporation into GlcNAc-1-P and UMP was slightly reduced under basal conditions in WT*rpoN* organisms decreased significantly upon itaconate exposure (Supplementary Fig. 3j). Overall the transcriptomic and carbon tracing studies demonstrate that the availability of itaconate to modify RpoN provides a coordinated enhancement of the fundamental metabolic activities required for bacterial proliferation, promoting successful *P. aeruginosa* infection in a setting of inflammation and oxidant stress.

RpoN 218/275 cysteines are conserved in clinical isolates

Our findings thus far indicate that post-translational modification of RpoN by itaconate enhances the ability of the organisms to establish pulmonary infection by optimizing bacterial metabolic activity, as modeled by the laboratory standard strain PAO1. Although *rpoN* is an

https://doi.org/10.1038/s41467-025-67153-1

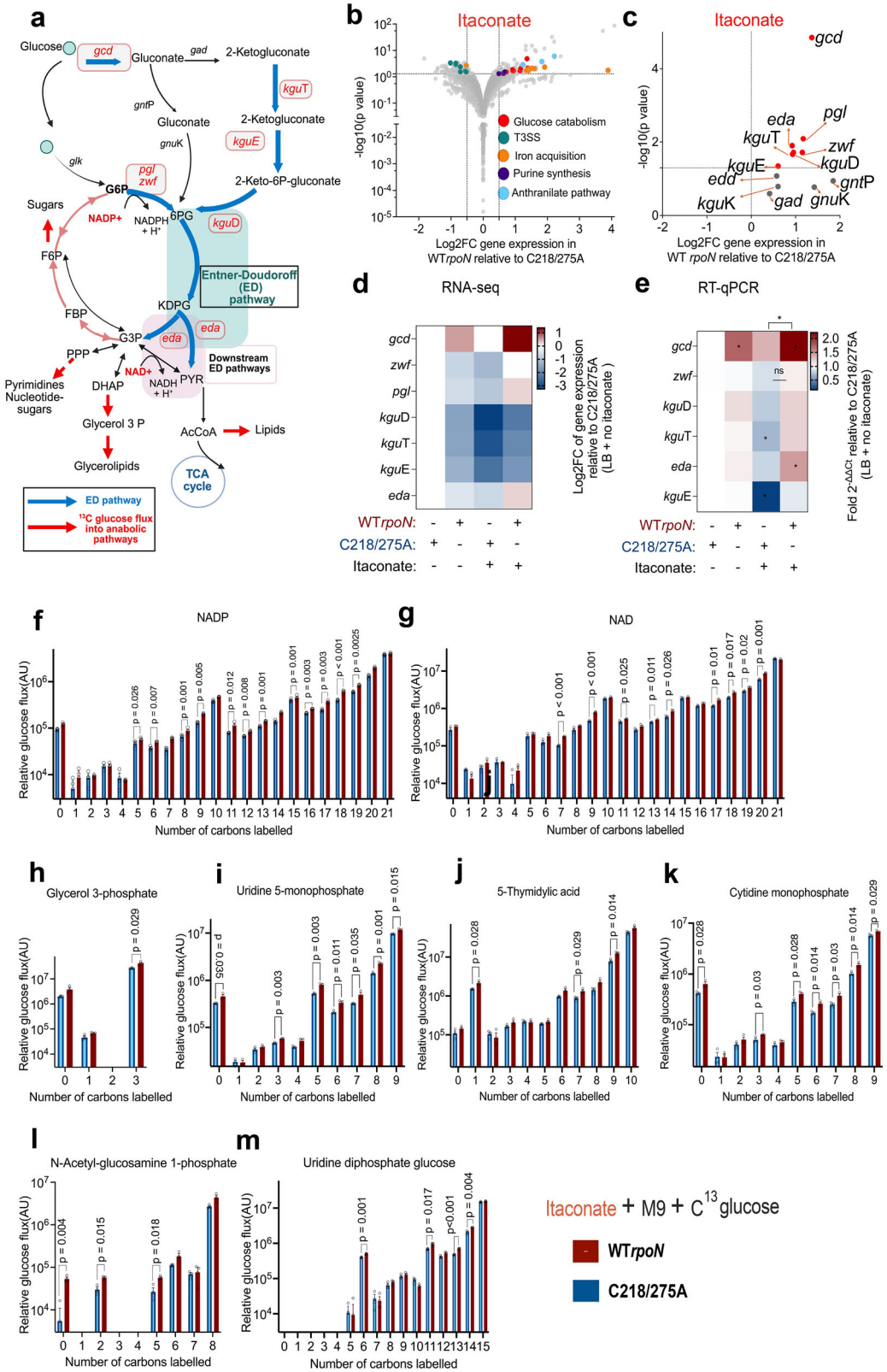

essential gene[15], it is a site of mutation in clinical isolates[25]. We postulated that the cysteine residues at 218 and 275 in RpoN would be highly conserved in *P. aeruginosa* from patients with pneumonia if they are biologically important to enable infection amidst phagocytes and itaconate stress. We analyzed *rpoN* sequences in publically available data sets from clinical isolates of *P. aeruginosa*, known to associated with either acute ICU or chronic (cystic fibrosis (CF) pulmonary infection (Fig. 4a). We identified several mutations in the clinical isolates, mostly synonymous variants, a few missense mutations, or deletions. The frequency of mutations was significantly greater in isolates from long standing CF infection than in the ICU isolates (Fig. 4b). A comparison of the *rpoN* genomic sequences and predicted proteins from these different datasets indicated conservation of the cysteine residues in the same location as in the reference PAO1 sequence (Fig. 4c). This is a

Fig. 3 | Impact of RpoN S-itaconation on transcriptional profile and anabolic glucose utilization in *P. aeruginosa*. **a** Schematic of glucose metabolism in *P. aeruginosa*, highlighting RpoN S-itaconation prevents repression of genes (red) involved in the gluconate and Entner–Doudoroff (ED) pathways (blue), as well as enhanced glucose flux into anabolic product formation (red arrows) from primary metabolic pathways in WT *rpoN* versus C218/275A strains grown with itaconate. **b** Bulk RNA seq to determine differentially expressed genes in WT *rpoN* relative to C218/275A grown in LB media with itaconate. Grey dots represent all genes; colored dots represent genes of specific pathways. *Y* axis: logarithmic scale, cut off set on *Y* axis: −log10 (*p* value) ≥ 1.3; cut off set on *X* axis Log2FC (Fold change) > 1. **c** Volcano plot of differentially expressed genes specific to gluconate or ED pathway in presence of itaconate. Significantly expressed genes associated with gluconate and ED pathways as determined by **d** RNA seq ($n = 2$) and **e** RTqPCR ($n = 6$) in WT*rpoN* relative to C218/C275A with or without itaconate. Effect of itaconate on the ^{13}C glucose carbon abundance in different isotopologues of metabolites in WT*rpoN* relative to C218/C275A ($n = 3$). Enrichment of ^{13}C glucose into isotopologues of (**f**, **g**) cofactors: NAD (C7 $p < 0.001 = 0.0003$; C9 $p < 0.0001 = 5.7988E\text{-}05$) and NADP, (**h**) glycerol, (**i**–**k**) pyrimidines: UMP, CMP, dTMP, and (**l**, **m**) sugars (**m**, C13 $p < 0.001 = 0.00037$). Data are presented as mean ± s.e.m. Significance is determined by Wald *t*-test (**b**–**d**) and Unpaired two-tailed Student's *t*-test (**e**, **f**–**m**). ns non-significant and * (significant) * (**e**) C218/275 A vs WT*rpoN* (*p* value for *gcd* = 0.042); C218/275A vs C218/275A itaconate (*p* values for *kguT* = 0.008, *kguE* = 0.0107); C218/275A vs WT*rpoN* itaconate (*p* values for *gcd* = 0.0004, *eda* = 0.0395); C218/275A itaconate vs WT*rpoN* itaconate (*p* values for *gcd* = 0.0164, kguD = 0.0164, kguT = 0.0275, kguD = 0.0015, *eda* = 0.015). Schematics in (**a**) is created in BioRender. Beg, A. (2025) https://BioRender.com/l3jqdlq. All statistical tests are two-sided. Source data are provided as a Source Data file 3.

region of RpoN expected to be involved in RNA polymerase binding[18], outside of the canonical DNA binding domain associated with the σ^{54} −12 and −24 regions of target genes (Fig. 4d, e). As depicted in the ribbon diagrams, mutations in the clinical strains did not appear likely to involve critical regions of RpoN, those involved in RNAP interactions or DNA recognition sites (Fig. 4d), although they could affect interactions with enhancer binding proteins[26]. The conservation of cysteines at positions 218 and 275 across the *P. aeruginosa* isolates from pneumonia patients worldwide is consistent with the physiologic role of S-itaconation of RpoN to promote the pathogenesis of *P. aeruginosa* pulmonary infection.

Discussion

The goal of this study was to establish how *P. aeruginosa* senses and responds to aspiration into the lung, an oxidant-rich environment replete with phagocytes and their products. Aided by decades of accumulated data characterizing the metabolic and genetic properties of this ubiquitous pathogen, we identified the alternative σ^{54} factor RpoN as highly responsive to the phagocyte-specific immunometabolite itaconate, which seems especially biologically appropriate. Whereas the importance of itaconate in regulating innate immune responses to pathogens is increasingly appreciated[7,8,14], its impact on bacteria as one of the most abundant metabolites in the infected airway, has been less well appreciated. Upon sensing itaconate, genes directing its transport and assimilation, as well as *rpo*N expression itself, are all upregulated. We found that *P. aeruginosa* limits itaconate toxicity by covalent binding to cysteine residues of RpoN and that itaconated RpoN boosts bacterial metabolism by promoting use of the preferred Entner–Doudoroff Pathway to generate ATP. The itaconated transcription factor also enhances the production of NAD and NADP co-factors utilized in this pathway by increasing expression of the anthranilate-tryptophan-kyrenurine cascade. Thus, WT *P. aeruginosa* responds to the challenges of itaconate through effects on a global transcription factor. It is striking, but not surprising, that a host-specific immunometabolite has such a major impact promoting *P. aeruginosa* infection.

Our data emphasize the importance of *rpoN*, a bacterial gene not typically considered a virulence factor in the pathogenesis of pulmonary infection. The expression of *rpoN* contributes to the exceptional metabolic versatility of *P. aeruginosa*. While the pathogens can metabolize itaconate, the S-itaconation of RpoN confers more pervasive benefits to support persistence in the oxidant-rich lung. Itaconated RpoN by promoting the generation and utilization of gluconate, which accumulates in cystic fibrosis patients with pulmonary infection[20], optimizes ATP production in settings in which glucose is limited, such as the airway[27], a likely consequence of substrate competition from neutrophils[22,28]. Utilization of the Entner–Doudoroff pathway and production of NADP also increases protection from oxidants via glutathione and generates less ROS itself than glycolysis. Thus, as an in vivo response to the challenges of survival in the lung, the ability of these pathogens to exploit host itaconate helps to explain their success as opportunistic pathogens. As other Gram-negative bacteria and members of the *ESKAPE* family[29] express *rpoN* with conserved cysteine residues in a similar configuration as *P. aeruginosa*, strategies to prevent bacterial adaptation to the itaconate-dominated milieu of the infected lung by interfering with RpoN might prove more useful than the development of vaccines targeting individual gene products[30].

Methods

Mouse experiments

All animal experiments were conducted in accordance with institutional guidelines at Columbia University Irving Medical Center and approved under IACUC protocol AABD5602. Wild-type (WT) C57BL/6NJ mice (7–8 weeks old, 20–25 × *g*; Jax #005304) were obtained from the Jackson Laboratory. Irg1$^{-/-}$ (Acod1$^{-/-}$) mice (Jax #029340) were also obtained from the Jackson Laboratory and bred in-house at Columbia University Irving Medical Center. Both WT and Irg1$^{-/-}$ mice were immunocompetent and did not receive any medical or drug treatments prior to infection. Each in vivo experiment included an equal number of male and female mice (50:50 ratio), and no sex-based differences were anticipated. Animals were randomly assigned to cages and housed in barrier facilities under standard conditions (12-h light/dark cycle, temperature 18–23 °C, 30–50% humidity). Mice were fed a regular irradiated chow diet (Purina Cat #5053, distributed by Fisher).

Key reagents

Dream Taq PCR mastermix (K1081, Thermo Scientific™), EcoRI-HF (NEB R0101S) and HindIII-HF(NEB, R3104S), QIAprep Spin Miniprep Kit (QIAGEN, 27104), T4 DNA Ligase (5 U/μL) (Thermo Scientific™, EL0011), ReliaPrep™ DNA Clean-Up and Concentration System (Promega A2893).

Tetracycline hydrochloride (Sigma, T7660), Itaconate (Sigma# I29204), D-(+)-Glucose (Sigma-Aldrich, G8270), M9 minimal media (Gibco™A1374401), Seahorse calibrant (Agilent #100840-000).

RNAprotect Bacteria Reagent (QIAGEN, 76506), Proteinase K (QIAGEN, 19131), TRK lysis buffer (Omega Bio-tek, R6834-02), Multiscribe Reverse Transcriptase (Applied Biosystems, 43-688-14), PowerUp SYBR Green Master Mix (Applied Biosystems, 25742), DNA-free™ DNA Removal Kit (Invitrogen, AM1906).

Antibodies and staining reagents: Anti-CD45-AF700 (BioLegend, 103127), anti-CD11b-AF594 (BioLegend, 101254), anti-CD11c-BV605 (BioLegend, 117334), anti-SiglecF-AF647 (BD, 562680), anti-MHCII-APC-Cy7 (BioLegend, 107628), anti-Ly6C-BV421 (BioLegend, 128032), and anti-Ly6G-PerCP-Cy5.5 (BioLegend, 127616), LIVE/DEAD viability dye (Invitrogen, L23105A), 15.45 μm DragonGreen, Bangs Laboratories Inc., FS07F).

Growth condition of bacterial strains

P. aeruginosa strains—PAO1, Δ*rpoN*, Δ*rpoN*:p*rpoN*, Δ*rpoN*:pC218/C275, Δ*rpoN* empty vector control (EVC) were used pHERD26T. In the

https://doi.org/10.1038/s41467-025-67153-1

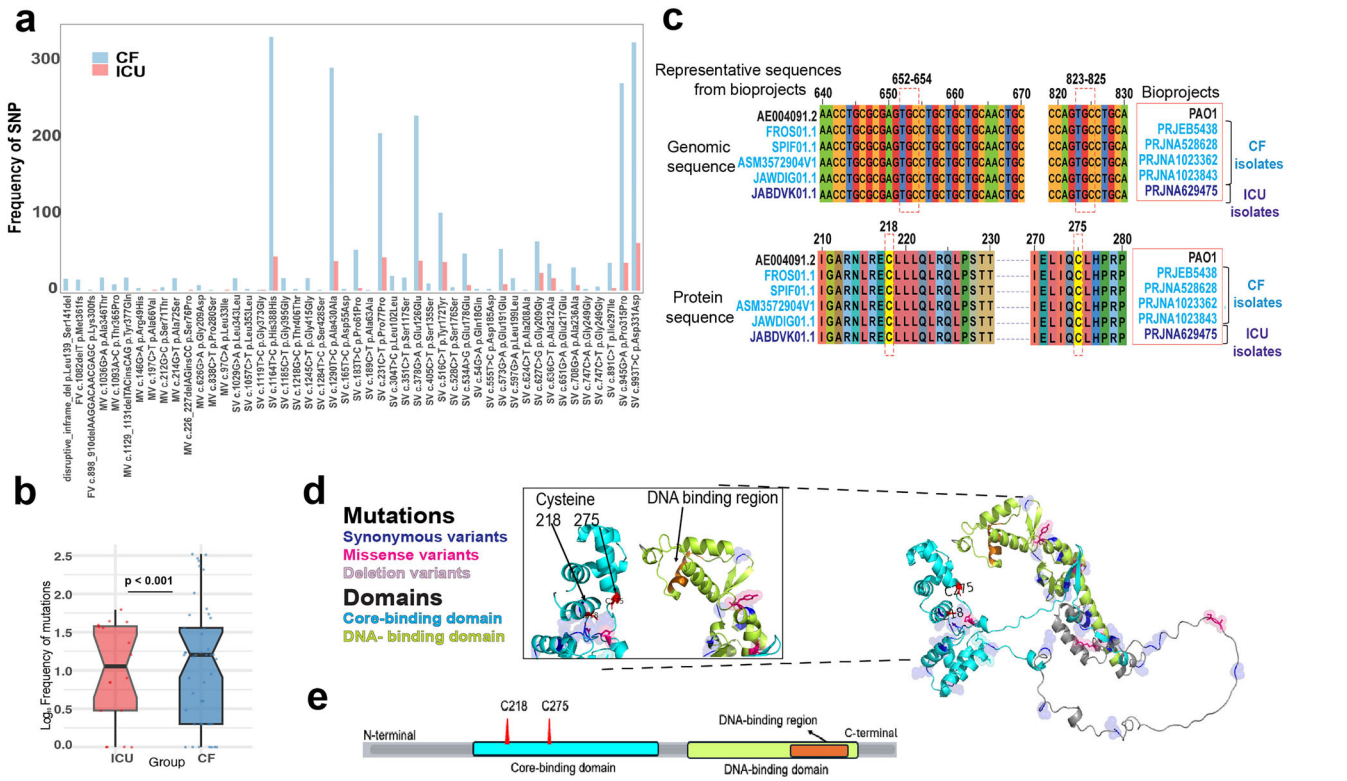

Fig. 4 | Clinical isolates conserve RpoN cysteines modified by itaconate. **a** Relative frequency of mutations in the *rpoN* gene of *P. aeruginosa* strains from CF ($n = 374$) and ICU patients ($n = 62$) isolates (SV synonymous variant, MV missense variant). **b** Box-plot representing the significant difference in frequency of total mutations in *rpoN* gene among CF ($n = 374$) and ICU ($n = 62$) groups. The plot shows median values (ICU = 1.05, CF = 1.20), interquartile range (IQR) (ICU = 0.48–1.58, CF = 0.30–1.56), whiskers representing minimum and maximum within 1.5 × IQR (ICU = 0–1.79, CF = 0–2.52), notches for 95% confidence interval of the median (ICU = 0.64–1.46, CF = 0.91–1.50), and points as outliers beyond the whiskers. **c** Alignment of *rpoN* sequences from representative datasets (labeled by source BioProject number), highlighting the conservation of cysteines at positions 218 and 275, relative to PAO1, at both genomic (652–654; 823–825) and protein (218/275) sequence levels. (Bioprojects: CF-blue; ICU: purple). **d** Ribbon structure of RpoN protein illustrating different mutations and domains, **(inset)** position of conserved cysteines 218/275 relative to DNA binding region of RpoN. **e** Linear map of RpoN protein from N-C terminus, depicting positions of conserved cysteines, DNA-binding region, core- and DNA-binding domain. Shapiro–Wilk normality test identified data not normally distributed and significance was determined by Wilcoxon rank-sum test ($W = 489.5$, p-value = 7.13E-07) (**b**). All statistical tests are two-sided. Source data are provided as a Source Data file 4.

experiments, laboratory *Pseudomonas* strains were grown in LB for overnight and subcultured until exponential phase. All strains were streaked and maintained on LB agar plates, while Δ*rpoN*:p*rpoN*, Δ*rpoN*:pC218/C275, Δ*rpoN* (EVC) were maintained on LB agar plates supplemented with 50 μg/mL of tetracycline.

Strains and plasmids

Strains, plasmid, and primers used in this study are listed in Supplementary data 3. We constructed an *rpoN* mutant in which the codons for cysteines at positions 218 and 275 were substituted with alanine using the overlap extension PCR method[31]. The *rpoN* sequence was PCR-amplified using Dream Taq PCR mastermix (Thermo Scientific™, K1081) from genomic DNA of PAO1 WT using primer pairs, RpoN_F and RpoN_R. The mutation at 218 position was introduced using primer sets RpoN_F /218_R and 218_F/ RpoN_R, followed by fusion of resultant PCR products using RpoN_F and RpoN_R. Similarly, substitution mutation was introduced in C218A**rpoN* at 275 position using primer set RpoN_F/275_R and 275_F/RpoN_R, followed by fusion of resultant PCR products using RpoN_F and RpoN_R. The amplicons, *rpoN* and C218/275A**rpoN* were cloned into vector pHerd26T using EcoRI-HF (NEB R0101S) and HindIII-HF (NEB, R3104S), yielding plasmids pHerd26T-WT*rpoN* and pHerd26T-C218/C275A. Verified plasmids were electroporated into Δ*rpoN* PAO1, and Transformants were selected on LB agar plates supplemented with 50 μg/mL of tetracycline, as previously described[32]. Clones were screened by PCR using flanking primers RpoN_F and RpoN_R, followed by Sanger sequencing of the amplicons.

Mouse pneumonia model

Mouse pneumonia infection was carried out with 7–8 weeks old male and female (C57BL/NJ6 WT and *Irg1*$^{-/-}$ (*Acod1*$^{-/-}$) mice as previously described[14]. After anesthesia, animals were exposed to either PBS, WT PAO1, Δ*rpoN*, Δ*rpoN*:p*rpoN*, or Δ*rpoN*:pC218/C275. A 50 μL volume of ~10^6 CFUs of either *P. aeruginosa* strain or PBS alone (non-infected) was intranasally inoculated into the mice. Mice were euthanized at 16 h post-infection; whole lungs and BALF were collected aseptically. The lung was homogenized through 40 μm cell strainers (Falcon, 352340). Aliquots of BALF and lung homogenates were serially diluted and plated on LB agar plates (supplemented with 50 μg/mL tetracycline when needed) to determine the bacterial burden. The BALF and lung homogenates were spun down and the BALF supernatant was collected for cytokine and untargeted metabolomic analysis. After hypotonic lysis of the red blood cells, the remaining BALF and lung cells were prepared for fluorescence-activated cell sorting (FACS) analysis as described below. No calculation was used to determine the number of mice required. No data blinding was performed.

Flow cytometry for immune cell recruitment in infection studies

Immune cell profiling in BALF and lung tissue was performed by staining isolated cells with a LIVE/DEAD viability dye (Invitrogen,

L23105A) and a fluorescent antibody cocktail, along with 10 μL of counting beads (15.45 μm DragonGreen, Bangs Laboratories Inc., FS07F). The antibody panel included: anti-CD45-AF700 (BioLegend, 103127), anti-CD11b-AF594 (BioLegend, 101254), anti-CD11c-BV605 (BioLegend, 117334), anti-SiglecF-AF647 (BD, 562680), anti-MHCII-APC-Cy7 (BioLegend, 107628), anti-Ly6C-BV421 (BioLegend, 128032), and anti-Ly6G-PerCP-Cy5.5 (BioLegend, 127616), each diluted 1:200 in PBS. Staining was carried out for 1 h at 4 °C. After washing, cells were fixed in 2% paraformaldehyde (Electron Microscopy Sciences, 15714-S) and analyzed on a BD LSRII flow cytometer using FACSDiva v9 software. Data were processed with FlowJo v10. Cell populations were identified based on the following markers: Alveolar macrophages: $CD45^+$ $CD11b^{+/-}$ $SiglecF^+$ $CD11c^+$; Neutrophils: $CD45^+$ $CD11b^+$ $SiglecF^-$ $MHCII^-$ $CD11c^-$ $Ly6G^+$ $Ly6C^{+/-}$; Monocytes: $CD45^+$ $CD11b^+$ $SiglecF^-$ $MHCII^-$ $CD11c^-$ $Ly6G^-$ $Ly6C^{+/-}$. Gating strategy by FACS is provided in the Supplementary Fig. 4.

Cytokine analysis

Cytokine levels in mouse BALF supernatants were measured by Eve Technologies (Calgary, Canada) using bead-based multiplex technology.

Untargeted metabolomic analysis

Metabolite profiling of BALF samples was conducted using high-resolution LC-MS at the Calgary Metabolomics Research Facility (Calgary, Canada). Metabolite extraction was performed using a 50% methanol (Supelco #106018) and water (v/v) solution. LC-MS analysis was carried out on a Q Exactive HF Hybrid Quadrupole-Orbitrap mass spectrometer (Thermo Fisher Scientific) coupled to a Vanquish UHPLC system (Thermo Fisher Scientific). Chromatographic separation was conducted on a Syncronis HILIC UHPLC column (2.1 mm × 100 mm × 1.7 μm, Thermo Fisher Scientific) using a binary solvent system at a flow rate of 600 μL/min. Solvent A was 20 mM ammonium formate at pH 3 in mass spectrometry-grade water, and solvent B was mass spectrometry-grade acetonitrile containing 0.1% formic acid (v/v). The gradient program was as follows: 0–2 min, 100% B; 2–7 min, 100%–80% B; 7–10 min, 80%–5% B; 10–12 min, 5% B; 12–13 min, 5%–100% B; 13–15 min, 100% B. A 2 ml of sample was injected. The mass spectrometer operated in negative full-scan mode at a resolution of 240,000, scanning from 50 to 750 m/z. Metabolites were identified by matching observed m/z values (±10 ppm) and retention times with those of commercial metabolite standards (Sigma-Aldrich). Data analysis was conducted using E-Maven v0.10.0.

Isolation of bacterial RNA

WT*rpoN* and C218/C275 strains were grown overnight in LB media (+50 μg/mL tetracycline). Overnight cultures were inoculated (1/100) into LB (+ 50 μg/mL tetracycline) with or without itaconate (Sigma# I29204) and were grown at 37 °C to late exponential phase. Approximately 2×10^8 *P. aeruginosa* cells were harvested by centrifugation, and the resulting pellet was resuspended in RNAprotect Bacteria Reagent (QIAGEN, 76506). The suspension was vortexed briefly and incubated at room temperature (RT) for 10 min before centrifugation. The bacterial pellets were then lysed in a buffer pH 8.0 (containing 30 mM Tris (Corning, 46-030-CM), 1 mM EDTA (Thermo Fisher Scientific, 1861283), 15 mg/mL lysozyme (Sigma, L6876), and 200 mg/mL proteinase K (QIAGEN, 19131)), with incubation at RT for 10 min. Following lysis, TRK lysis buffer (Omega Bio-tek, R6834-02) and 70% ethanol (v/v) were added to the mixture. The lysates were then applied to E.Z.N.A. RNA isolation columns (Omega Bio-tek), and total RNA was extracted according to the manufacturer's protocol. Residual genomic DNA was removed by DNase treatment using the DNA-free™ DNA Removal Kit (Invitrogen, AM1906).

Complementary DNA (cDNA) synthesis and qRT–PCR

Complementary DNA (cDNA) was synthesized from RNA using Multiscribe Reverse Transcriptase (Applied Biosystems, 43-688-14). Quantitative real-time PCR was carried out with gene-specific or housekeeping primers as listed in Supplementary data 3, PowerUp SYBR Green Master Mix (Applied Biosystems, 25742), and the StepOnePlus Real-Time PCR System (Applied Biosystems). Relative gene expression levels were calculated using the ΔΔCt (delta-delta Ct) method.

Bulk RNA sequencing

Bacterial RNA was extracted as previously described. A ribosomal RNA (rRNA)-depleted cDNA library was prepared according to the manufacturer's instructions using the Universal Prokaryotic RNA-Seq Prokaryotic AnyDeplete kit (NuGEN #0363-32) and sequenced with Illumina HiSeq. Raw base call files were converted to fastq format using Bcl2fastq. Quality-filtered reads were then aligned to the *P. aeruginosa* PAO1 reference genome (RefSeq: GCF_000006765.1) using STAR Aligner v2.7.3a. Aligned reads were annotated with read group information and duplicate reads were identified using Picard Tools v2.22.3. Quantification of raw counts was performed using FeatureCounts from the Subread package v1.6.3. Differential gene expression analysis was conducted using DESeq2 in R v3.5.3 and low-abundant transcript having threshold of 3 reads per gene were excluded in the analysis. The bacterial transcriptional data were plotted as a volcano plot heatmap plot using GraphPad Prism (v10.0c).

^{13}C glucose labeling and stable isotope tracing

WT*rpoN* and C218/C275 strains were grown overnight in LB media (+50 μg/mL tetracycline) with or without 20 mM of itaconate. The overnight cultures were washed and resuspended in the same volume of M9 minimal media (Gibco™A1374401). The cultures were inoculated (1/50) into M9 minimal media supplemented with 7.5 mM of ^{13}C glucose (Sigma #389374) (+50 μg/mL tetracycline) and grown at 37 °C to late exponential phase. For metabolite extraction, each culture was pelleted and washed with PBS twice centrifuged in 2000 × *g* for 10 min at 1 °C. The pellets were resuspended in a 3:1 methanol:water extraction solution and lysed with 10 freeze-thaw cycles by alternating emersion in liquid nitrogen and a dry-ice/ethanol bath. The debris was removed by centrifugation at 14,000 × *g* for 5 min at 1 °C and the supernatant was stored for analysis. Targeted LC/MS analysis was performed on a Q Exactive Orbitrap mass spectrometer (Thermo Scientific) coupled to a Vanquish UPLC system (Thermo Scientific). The Q Exactive operated in polarity-switching mode. A Sequant ZIC-HILIC column (2.1 mm i.d. × 150 mm, Merck) was used for separation of metabolites. Flow rate was set at 150 μL/min. Buffers consisted of 100% acetonitrile for mobile A, and 0.1% NH_4OH/20 mM CH_3COONH_4 in water for mobile B. Gradient ran from 85 to 30% A in 20 min followed by a wash with 30% A and re-equilibration at 85% A. Metabolites were identified based on exact mass within 5 ppm and standard retention times. Relative quantitation was performed based on peak area for each isotopologue. All data analysis was done using MAVEN 2011.6.17.

In situ itaconation profiling of cysteines in *P. aeruginosa*

Cysteines in proteome subjected to S-itaconation were identified using the workflow described here[10] with $n = 3$ samples. *P. aeruginosa* PAO1 were grown in LB media at 37 °C to stationary phase. Cultures were washed and resuspended in pre-chilled PBS. Where 800 μL of *P. aeruginosa* PAO1 suspension in PBS was treated without or with 80 μL pH-adjusted itaconate, was incubates on the ThermoMixer (950 rpm, 1 h, 37 °C, 30 min). Both groups were then incubated with 8 μL of the C3A probe (950 rpm, 37 °C, 1 h). Cells were pelleted, washed, resuspended in 1 mL of 0.1% PBST, and lysed. Lysates were clarified by

centrifugation, and the supernatant was transferred to fresh tubes. After competition, both groups were incubated with 8 mL of the C3A probe on the ThermoMixer (950 rpm, 37 °C, 1 h). Bacteria were pelleted, washed, and resuspended in 1 mL of 0.1% PBST for lysis. Lysates was centrifuged (20,000 × *g*, 10 min, RT) to remove the debris and the supernatants was transferred into a new tubes. Click reaction was carried out at 29 °C for 1 h (1200 rpm)on a Thermomixer with 106 µL of Click reagent mix comprising of: 60 µL TBTA ligand, 20 µL 50 mM $CuSO_4$, 20 µL freshly prepared 50 mM TCEP, and 6 µL 20 mM acid-cleavable azide-biotin tag (Confluore). The click-labeled lysates were precipitated by 5 mL of MeOH/chloroform (4:1) and 3 mL of ddH2O. Precipitates were washed twice with pre-chilled MeOH, resuspended in 1 mL of 1.2% SDS in PBS, followed by sonication, heating for 10 min at 90 °C, and centrifuged (20,000 × *g*, 10 min, RT) to remove excessive copper. Supernatants were combined with the pre-washed streptavidin beads (Thermo Fisher) and incubated for 4 h at 29 °C. Beads were washed PBS three times and ddH2O three times, followed by resuspension in 500 mL of 8 M urea (Sigma)/100 mM TEAB (Sigma). The samples were reduced on ThermoMixer (1200 rpm, 30 min, 37 °C) by 25 mL of 200 mM DTT (Shanghai Yuanye Bio-Technology Co., Ltd) and alkylated on the ThermoMixer (1200 rpm, 30 min, 35 °C) by 25 mL of 400 mM 2-iodoacetamide (Sigma). The beads were then resuspended in resuspended in 200 mL of 2 M urea/100 mM TEAB containing 1 mM CaCl2 and 10 ng mL1 trypsin (Promega) for digestion on ThermoMixer (1200 rpm, 30 min, 35 °C). Post-digestion, the supernatants were carefully transferred into a new 1.5 mL Protein LoBind Tubes (Eppendorf). The beads were washed, and post-washed supernatants were pooled with primary digest. The digested peptides were subjected to mass spectrometry for identification of itaconation of cysteines.

Genomic analysis of clinical isolates

Publicly available whole genome sequences for *Pseudomonas* CF isolates (Bioproject accession number: PRJEB5438, PRJNA528628, PRJNA1023362, PRJNA1023843 on NCBI) and ICU isolates (ENA accession number: PRJNA629475) were used for mutation analysis with respect to the reference genome PAO1 (Genomics accession no.: AE004091.2).SNPs in *rpoN* were identified in CF and ICU isolates of *P. aeruginosa* using Snippy v4.6.0 (https://github.com/tseemann/snippy), with the PAO1 genome as the reference. The detected variants, including SNPs and indels, were visualized using Jalview for comparative sequence analysis to determine the conservation of cysteines residues at the codon and protein sequence level. Representative sequences of *rpoN* from each bioprojects with respect to reference PAO1 were used to represent conservation of cysteine residues.

Extracellular flux analysis

WT*rpoN*, C218/C275, and Δ*rpoN* strains were grown in LB overnight, then washed twice with filtered PBS before inoculating (1×10^7) into 450 µl of 1× of M9 minimal media supplemented with 2 mM of $MgSO_4$ and 0.1 mM of $CaCl_2$ in Seahorse XFe24 cell culture plate (Agilent #102334-000B). 50 µl of 75 mM glucose or 200 mM itaconate in M9 media was loaded onto the Seahorse XFe24 cartridge, which was previously hydrated in Seahorse calibrant (Agilent #100840-000) overnight at 37 °C. After 60 min of stabilization at the basal state, glucose or itaconate was acutely injected into the plate to achieve the final concentration of 7.5 mM or 20 mM, respectively. Bacterial extracellular acidification and oxygen consumption rates were captured with Seahorse XFe24 Analyzer (Agilent #1002238-100) using Seahorse Wave Desktop v2.6.0.

Biofilm quantification

A clear, flat-bottom 96-well plate (Greiner, #M2936) was prepared using either LB or M9 minimal medium supplemented with 0.5% (w/v) glucose, with or without 20 mM itaconate. Each well was inoculated with 1×10^8 CFU of *P. aeruginosa* strains (WT *rpoN*, C218/275 A mutant, or Δ*rpoN*) and incubated statically at 37 °C for 24 h (or 48 h for M9 + glucose conditions). Bacterial growth was monitored by measuring optical density at 600 nm (OD_{600}) using SkanIt Software 7.0 RE. For biofilm staining, the supernatant was carefully removed, wells were washed and air-dried, and biofilms were fixed with 100% methanol. Biofilms were then stained with 1% crystal violet. After removing the stain, plates were washed, dried, and the biofilm was solubilized in 33% acetic acid. Absorbance at 540 nm was measured using a Varioskan Lux plate reader (Thermo Scientific, #3020-82355).

Growth curves

Growth assays for bacterial growth curves, a U-bottomed, clear 96-well plate (Greiner Bio-One, 650161) was prepared with 198 µL of M9 minimal media supplemented with glucose and/or succinate, itaconate. Each well was inoculated with 2 µL overnight bacterial culture grown in LB with or without 20 mM itaconate, standardized to an OD600nm of 4. Absorbance at 600 nm was read every 10 min for 18 h on the SpectraMax M2 plate reader (Molecular Devices), as the plate incubated at 37 °C with shaking.

Swarming motility

Swarming assays were conducted following a previously established protocol[33], using LB medium supplemented with 0.5% (w/v) agar. Once solidified, the plates were briefly air-dried at room temperature and spot-inoculated with 2 µL of overnight LB cultures. Plates were incubated face-up in stacks of no more than two at 37 °C for 18 h. Swarming motility was assessed by measuring the diameter of the swarming zone.

Protein structure

The three-dimensional structure of the *P. aeruginosa* RpoN protein was predicted using AlphaFold 3. PyMOL™ version 3.0.4 (Schrödinger, LLC) software was used to visualize and perform the structural mapping of domains, conserved cysteine residues, and mutations.

Statistical analysis

Experiments in this study were not conducted in a blinded manner. All statistical analyses and graphing were performed using GraphPad Prism 9. Graphical data are presented as mean ± SEM, under the assumption of a normal distribution. For comparisons involving more than two groups, one-way ANOVA followed by post hoc multiple comparisons was used. When analyzing two or more groups over time, two-way ANOVA with post hoc testing was applied. Differences between two groups were assessed using parametric tests (Student's *t*-test or ANOVA) when data were normally distributed, or nonparametric tests (Mann–Whitney or Kruskal–Wallis) when normality could not be assumed. A two-tailed *P* value of <0.05 was considered statistically significant. Specific *P* values, along with the number of independent experiments and replicates, are provided in the figure legends.

Reporting summary

Further information on research design is available in the Nature Portfolio Reporting Summary linked to this article.

Data availability

The MS proteomics data have been deposited at the ProteomeXchange Consortium (http://proteomecentral.proteomexchange.org) via the iProX partner repository. Chemoproteomic profiling data is deposited under ProteomeXchange ID: PXD050510, with the iProx project ID: IPX0008134000 and Subproject ID: IPX0008134002 for RpoN MS data. Dual RNA seq and ^{13}C glucose labeling data as well as other data used in the paper are included in the supplementary data.

The whole genome sequencing and SNP results are provided in the source data file. Source data are provided with this paper.

References

1. Qin, S. et al. *Pseudomonas aeruginosa*: pathogenesis, virulence factors, antibiotic resistance, interaction with host, technology advances and emerging therapeutics. *Signal Transduct. Target. Ther.* **7**, 199 (2022).
2. Chen, Y.-T. et al. A host-pathogen metabolic synchrony that facilitates disease tolerance. *Nat. Commun.* **16**, 3729 (2025).
3. Heurlier, K., Denervaud, V., Pessi, G., Reimmann, C. & Haas, D. Negative control of quorum sensing by RpoN (sigma54) in *Pseudomonas aeruginosa* PAO1. *J. Bacteriol.* **185**, 2227–2235 (2003).
4. Shao, X. et al. The transcriptional regulators of virulence for *Pseudomonas aeruginosa*: therapeutic opportunity and preventive potential of its clinical infections. *Genes Dis.* **10**, 2049–2063 (2023).
5. Mould, D. L., Stevanovic, M., Ashare, A., Schultz, D. & Hogan, D. A. Metabolic basis for the evolution of a common pathogenic *Pseudomonas aeruginosa* variant. *Elife* **11**, e76555 (2022).
6. Zhao, K. et al. Evolution of lasR mutants in polymorphic *Pseudomonas aeruginosa* populations facilitates chronic infection of the lung. *Nat. Commun.* **14**, 5976 (2023).
7. O'Neill, L. A. J. & Artyomov, M. N. Itaconate: the poster child of metabolic reprogramming in macrophage function. *Nat. Rev. Immunol.* https://doi.org/10.1038/s41577-019-0128-5 (2019).
8. Peace, C. G. & O'Neill, L. A. The role of itaconate in host defense and inflammation. *J. Clin. Invest.* **132**, e148548 (2022).
9. McGettrick, A. F., Bourner, L. A., Dorsey, F. C. & O'Neill, L. A. J. Metabolic messengers: itaconate. *Nat. Metab.* **6**, 1661–1667 (2024).
10. Liu, Z., Liu, D. & Wang, C. In situ chemoproteomic profiling reveals itaconate inhibits de novo purine biosynthesis in pathogens. *Cell Rep.* **43**, 114737 (2024).
11. Mills, E. L. et al. Itaconate is an anti-inflammatory metabolite that activates Nrf2 via alkylation of KEAP1. *Nature* **556**, 113–117 (2018).
12. Lampropoulou, V. et al. Itaconate links inhibition of succinate dehydrogenase with macrophage metabolic remodeling and regulation of inflammation. *Cell Metab.* **24**, 158–166 (2016).
13. Riquelme, S. A. & Prince, A. Airway immunometabolites fuel *Pseudomonas aeruginosa* infection. *Respir. Res.* **21**, 326 (2020).
14. Riquelme, S. A. et al. *Pseudomonas aeruginosa* utilizes host-derived itaconate to redirect its metabolism to promote biofilm formation. *Cell Metab.* **31**, 1091–1106 e1096 (2020).
15. Shao, X. et al. RpoN-dependent direct regulation of quorum sensing and the type VI secretion system in *Pseudomonas aeruginosa* PAO1. *J. Bacteriol.* **200**, 00205–00218 (2018).
16. Huang, Q. et al. Structural and functional characterization of itaconyl-CoA hydratase and citramalyl-CoA lyase involved in itaconate metabolism of *Pseudomonas aeruginosa*. *Structure* **32**, 941–952. e943 (2024).
17. Qin, W. et al. Chemoproteomic profiling of itaconation by bioorthogonal probes in inflammatory macrophages. *J. Am. Chem. Soc.* **142**, 10894–10898 (2020).
18. Casaz, P., Gallegos, M. T. & Buck, M. Systematic analysis of sigma54 N-terminal sequences identifies regions involved in positive and negative regulation of transcription. *J. Mol. Biol.* **292**, 229–239 (1999).
19. Berger, A. et al. Robustness and plasticity of metabolic pathway flux among uropathogenic isolates of *Pseudomonas aeruginosa*. *PLoS ONE* **9**, e88368 (2014).
20. Behrends, V. et al. Metabolite profiling to characterize disease-related bacteria: gluconate excretion by *Pseudomonas aeruginosa* mutants and clinical isolates from cystic fibrosis patients. *J. Biol. Chem.* **288**, 15098–15109 (2013).
21. Daddaoua, A., Corral-Lugo, A., Ramos, J. L. & Krell, T. Identification of GntR as regulator of the glucose metabolism in *Pseudomonas aeruginosa*. *Environ. Microbiol.* **19**, 3721–3733 (2017).
22. El Husseini, N. et al. Characterization of the Entner-Doudoroff pathway in *Pseudomonas aeruginosa* catheter-associated urinary tract infections. *J. Bacteriol.* **206**, e0036123 (2024).
23. Knoten, C. A., Hudson, L. L., Coleman, J. P., Farrow, J. M. 3rd. & Pesci, E. C. KynR, a Lrp/AsnC-type transcriptional regulator, directly controls the kynurenine pathway in *Pseudomonas aeruginosa*. *J. Bacteriol.* **193**, 6567–6575 (2011).
24. Kurnasov, O. et al. NAD biosynthesis: identification of the tryptophan to quinolinate pathway in bacteria. *Chem. Biol.* **10**, 1195–1204 (2003).
25. Smith, E. E. et al. Genetic adaptation by *Pseudomonas aeruginosa* to the airways of cystic fibrosis patients. *Proc. Natl. Acad. Sci. USA* **103**, 8487–8492 (2006).
26. Zhang, N. & Buck, M. A perspective on the enhancer dependent bacterial RNA polymerase. *Biomolecules* **5**, 1012–1019 (2015).
27. Baker, E. H. & Baines, D. L. Airway glucose homeostasis: a new target in the prevention and treatment of pulmonary infection. *Chest* **153**, 507–514 (2018).
28. Tomlinson, K. L. et al. *Staphylococcus aureus* stimulates neutrophil itaconate production that suppresses the oxidative burst. *Cell Rep.* **42**, 112064 (2023).
29. Ho, C. S. et al. Antimicrobial resistance: a concise update. *Lancet Microbe* **6**, 100947 (2025).
30. Young, C., Walzl, G. & Du Plessis, N. Therapeutic host-directed strategies to improve outcome in tuberculosis. *Mucosal Immunol.* **13**, 190–204 (2020).
31. Heckman, K. L. & Pease, L. R. Gene splicing and mutagenesis by PCR-driven overlap extension. *Nat. Protoc.* **2**, 924–932 (2007).
32. Choi, K.-H., Kumar, A. & Schweizer, H. P. A 10-min method for preparation of highly electrocompetent *Pseudomonas aeruginosa* cells: application for DNA fragment transfer between chromosomes and plasmid transformation. *J. Microbiol. Methods* **64**, 391–397 (2006).
33. Ha, D.-G., Kuchma, S. L. & O'Toole, G. A. Plate-based assay for swarming motility in *Pseudomonas aeruginosa*. In *Pseudomonas Methods and Protocols*, 67–72 (New York, NY: Springer New York, 2014).

Acknowledgements

This study was funded by NIH grants R01HL170129 (A.P.), R35HL135800 (A.P.), T32-5T32DK0076 (G.G.), S10OD020056 to the Columbia Center for Translational Immunology (CCTI) Flow Cytometry Core. We thank Alain Filloux and Luke P. Allsopp for providing WT PAO1 and Δ*rpoN* PAO1 strains. Metabolomics data were acquired at the Calgary Metabolomics Research Facility (CMRF), University of Calgary, and this facility is supported by the International Microbiome Centre and the Canada Foundation for Innovation under Grant CFI-JELF 34986. We thank Dr. Guoan Zhang, Director of the Proteomics and Metabolomics Core Facility at Weill Cornell Medicine for his help with bacterial metabolomics assays.

Author contributions

Conceptualization: A.P., A.Z.B. Methodology: A.Z.B., Y.T.C., T.W.F.L., S.R., A.P. Investigation: A.Z.B., Y.T.C., Z.L., G.G., J.M., T.W.F.L., A.T., L.F., L.D., I.L., C.W. Visualization: A.Z.B., Y.T.C. Funding Acquisition: A.P. Project Administration: A.P. Supervision: A.P. Writing–original draft: A.P. Writing–review editing: A.P., S.R., and A.Z.B.

Competing interests

The authors declare no competing interests.

Additional information

Supplementary information The online version contains supplementary material available at https://doi.org/10.1038/s41467-025-67153-1.

Correspondence and requests for materials should be addressed to Alice Prince.

Peer review information *Nature Communications* thanks the anonymous reviewer(s) for their contribution to the peer review of this work. A peer review file is available.